

Determination of the surface density of polyethylene glycol on gold nanoparticles by use of microscale thermogravimetric analysis

K. B. Sebyy · E. Mansfield

Received: 20 August 2014 / Revised: 15 January 2015 / Accepted: 27 January 2015 / Published online: 21 February 2015
© Springer-Verlag Berlin Heidelberg (outside the USA) 2015

Abstract The widespread integration of nanoparticle technologies into biomedicine will depend on the ability to repeatedly create particles with well-defined properties and predictable behaviors. For this to happen, fast, reliable, inexpensive, and widely available techniques to characterize nanomaterials are needed. Characterization of the surface molecules is particularly important since the surface, including the surface molecule density, plays a dominant role in determining how nanoparticles interact with their surroundings. Here, 10 and 30 nm gold nanoparticle NIST Standard Reference Materials were functionalized with fluorescently labeled polyethylene glycol (PEG) with either thiolate or lipoic acid anchoring groups to evaluate analytical techniques for determining surface coverage. The coating of the nanoparticles was confirmed with dynamic light scattering, microscale thermogravimetric analysis (μ -TGA), and ultraviolet–visible (UV–vis) spectroscopy. A UV–vis method for determining gold nanoparticle concentrations that takes into account spectral broadening upon functionalization was developed. The amount of bound PEG was quantified with μ -TGA, a technique analogous to thermogravimetric analysis that uses quartz crystal microbalances, and fluorescence spectroscopy of displaced ligands. It is shown that μ -TGA is a convenient technique for the quantification of ligands bound to inorganic particles while sacrificing a minimal amount of sample, and the treatment of

the functionalized nanoparticle dispersions with dithiothreitol may be insufficient to achieve complete displacement of the surface ligands for quantification by fluorescence measurements. The μ -TGA and fluorescence results were used to determine ligand footprint sizes—average areas occupied by each ligand on the particles' surface. The lipoic acid bound ligands had footprint sizes of 0.21 and 0.25 nm² on 10 and 30 nm particles, respectively while the thiolate ligands had footprint sizes of 0.085 and 0.18 nm².

Keywords Nanoparticle · Thermal analysis · Fluorescence

Introduction

Nanotechnology promises to radically transform medical treatments and diagnostics [1, 2], yet there are relatively few successful applications of nanotechnology to biomedicine. The ability to design effective and safe technologies for nanobiomedicine has been plagued by the inability to understand how nanoparticle properties relate to their in vivo behaviors. To uncover nanoparticle property–activity relationships, advancements need to be made in three fundamental areas [3]: techniques to rapidly measure particle properties [4–8], superior in vitro models that accurately replicate in vivo environments [9–12], and the ability to predict and monitor environment-dependent particle alterations [4, 13–16]. Not only will these advancements guide the design of nanoparticle systems used for biomedical purposes, but they will also provide information about the potential risks associated with incidental exposure of humans to nanoparticles from manufacturing, processing, and use in consumer products.

Contribution of NIST, an agency of the US government; not subject to copyright in the United States.

Electronic supplementary material The online version of this article (doi:10.1007/s00216-015-8520-x) contains supplementary material, which is available to authorized users.

K. B. Sebyy · E. Mansfield (✉)
Applied Chemicals and Materials Division, National Institute of Standards and Technology (NIST), Boulder, CO 80305, USA
e-mail: elisabeth.mansfield@nist.gov

Particle characterization has been identified as one of the major bottlenecks toward efficient commercialization of nano-enabled products [5, 17]. Even the most fundamental nanoparticle properties are not straightforward to measure and compare between laboratories; for example, size measurements can differ substantially, depending on the technique that is used [18]. Worse, some vital properties are often neglected completely. One such property is the determination of the number of molecules bound to the surface of inorganic particles. The behavior of nanoscale particles in biological environments is determined primarily by the molecules that are bound to their surfaces, since this surface layer forms the interface between the particle and its external environment [14, 19, 20]. Moreover, as the size of particles decrease to the nanoscale, the surface molecules become a sizeable fraction of the constituents that form the particle. The density of the ligands that are bound to the particle can affect many of the properties of the particles including their bio-distribution and cellular uptake when the ligands are active targeting groups; the stability of the particles for molecules that sterically stabilize the particles and inhibit access to their cores; and the potency of the particles when therapeutic compounds are bound to their surface.

Current methods to characterize the molecules on the surfaces of nanoparticles have been reviewed. [16, 17] These treatises described the measurement of surface molecules with nuclear magnetic resonance, Fourier-transform infrared spectroscopy, combustion elemental analysis, and traditional surface-analysis methods. As described in these reviews, such techniques are useful for determining the presence of bound functional groups, obtaining information about their structure, and determining relative amounts of bound ligands, but are only semi-quantitative for determining absolute numbers of bound molecules. Another approach is to measure the thickness of a surface molecule coating and presume a ligand structural model to calculate the density of surface molecules [21]. More direct quantitative techniques include fluorescence measurements [22, 23] and thermogravimetric analysis (TGA); [20, 24–28] however, both of these techniques suffer from serious shortcomings. Fluorescence measurements require intrinsically fluorescent ligands, or modification of the ligand with a fluorescent tag. This requirement severely limits the types of samples that can be dependably analyzed, since modified ligands may not accurately represent the true nature of unmodified ligands. Moreover, fluorescent ligands must be completely displaced and separated from gold particles to prevent fluorescence quenching by the gold core, and particle concentrations and ligand concentrations need to be measured independently. TGA is a fast and reliable method that determines the fractions of thermally stable and unstable masses of a sample. Provided that particle sizes and ligand molecular weights are well known, surface coverage for inorganic particles with combustible ligands can be calculated. The major

drawback of TGA for nanoparticle measurements is the large sample size required for analysis; a typical TGA experiment requires several milligrams of material, which makes it unfeasible to use for expensive or limited-quantity samples or for quality-control purposes when frequent and multiple experiments need to be made. In all cases, using multiple techniques to determine surface coverage is preferred to cross-validate results.

Recently, we reported the use of quartz crystal microbalances (QCMs) at elevated temperatures to mimic TGA with sample sizes of only a few micrograms. [29] Results from the QCM technique—henceforth referred to as μ -TGA— for carbon black, alumina, surfactants, and carbon nanotubes were shown to correlate well with data obtained with a TGA instrument. μ -TGA has also shown promise for nanoparticle characterization, because it uses far less sample than traditional TGA [8]. In this work, we confirm the addition of a polymer coating to gold nanoparticles with dynamic light scattering (DLS) and ultraviolet–visible spectroscopy (UV–vis) and apply μ -TGA and fluorescence spectroscopy to measure the amount of two different hetero-bifunctional polyethylene glycol (PEG) ligands bound to gold nanoparticles.

Gold nanoparticles are an important class of nanomaterials [3, 30, 31] with applications in drug delivery [7, 32–37], gene delivery [38–41], diagnostics [42, 43], and photothermal therapy [44, 45]. Because of the many promising applications for gold nanoparticles—which are already becoming realized [46]—and discrepancies between biological testing from different laboratories, the National Institute of Standards and Technology (NIST) has developed gold nanoparticle Standard Reference Materials [47] to help facilitate interlaboratory test comparisons. Well-characterized nanoparticles in conjunction with techniques to quantitatively measure molecules bound to the particle surface compose a powerful combination for studying the effects of surface density on particle behavior. Here, the PEG surface coverages of gold nanoparticle reference materials in two sizes—nominally 10 and 30 nm—were determined.

PEG was chosen for these studies because it is commonly used as a linker between functional components and nanoparticles, due to its well-known ability to stabilize nanoparticles, conceal them from the immune system, and resist non-specific absorption of biological molecules [2, 37, 48–51]. The PEG molecules used in this report consisted of a fluorophore attached to one end of the polymer, and either a thiol or lipoic acid anchoring group on the other end to bind the PEG to the gold surfaces. Lipoic acid attaches to gold through two gold-sulfur linkages while thiol facilitates single-point attachment. The fluorescently labeled PEG allows surface coverage to be measured by fluorescence in addition to μ -TGA. The mass-fraction information values of gold from the Reference Material Reports of Investigations [47] were used to calibrate UV–vis absorbance spectra to determine nanoparticle

concentrations. Knowledge of the size of particles from the Reports of Investigation and the molecular weight of PEG by matrix-assisted laser desorption/ionization time-of-flight mass spectrometry (MALDI-TOF-MS) enabled PEG footprint sizes to be calculated for both techniques. The use of two nanoparticle sizes and two anchoring groups allows for the effects of particle size and linker type on surface coverage to be determined.

Experimental [52]

Materials Dispersions of gold nanoparticle Standard Reference Materials in 30 nm (SRM 8012) and 10 nm (SRM 8011) sizes were obtained from NIST. All other chemicals were obtained from commercial sources. Lipoic acid-PEG-fluorescein isothiocyanate (LA-PEG-FITC) was made by reacting 1.6 mg of lipoic acid-PEG-amine (LA-PEG-NH₂, 3,400 g/mol) with fluorescein isothiocyanate (FITC, 0.4 mg in 40 μ L dimethylsulfoxide) in a 0.01 mol/L carbonate buffer, pH 9, to a final volume of 200 μ L. The reaction was allowed to proceed for 2 h. Unbound FITC was removed onto a 5 mL cross-linked dextran gel spin-column (85–260 μ m wet bead size, fractionation range: 1×10^3 – 5×10^3 g/mol). Thiol-PEG-FITC (HS-PEG-FITC, 3,400 g/mol) and thiol-PEG-methyl (HS-PEG-methyl, 5,000 g/mol) were purchased and used as received.

Before use, the 10 nm gold nanoparticles were passed through a 0.1 μ m aluminum oxide syringe filter, and the 30 nm gold nanoparticles were passed through a 0.45 μ m polyvinylidene fluoride syringe filter. Native citrate ligands on the gold nanoparticles were displaced with the PEG derivatives by combining 5.00 mL of the reference material with 1.5 mg to 4.0 mg of fluorescent PEG derivative dissolved in water in a volumetric flask. The four samples were diluted with water to a total volume of 10.00 mL, transferred to 15 mL polypropylene conical tubes, and protected from light. The reaction was allowed to proceed for 3 days at ambient temperature before the samples were separated from excess PEG and concentrated to a volume of less than 0.5 mL by at least three centrifugation cycles. The samples were purified further with dialysis (dialysis cassettes, 0.1 mL to 0.5 mL, 10,000 g/mol cut-off) against 1,000 mL of water until the fluorescence of the exchange water was equivalent to baseline measurements (usually three exchanges). The expected large stoichiometric excess of PEG for all of the samples was confirmed by the intense fluorescence of the supernatants that were removed after centrifugation.

Dynamic light scattering DLS experiments were performed on a Zetasizer Nano ZS (Malvern Instruments Ltd., Worcestershire, UK) with a scattering angle of 173° at

20 °C. The samples were diluted to have a maximum absorbance value near 0.1 and were measured in a low-volume quartz cuvette. The cumulants method was used to determine the Z-average hydrodynamic diameters of the particles. A minimum of five measurements were made of each sample with approximately 12 sub-runs per measurement.

UV-vis UV-visible spectroscopy was used to determine the concentration of gold nanoparticles. All measurements were made on a LAMBDA 1050 spectrometer (PerkinElmer, Waltham, MA) fitted with a three-detector module. Standard curves were created before and after passing the particles through syringe filters, and absorbance values were related to data from the Standard Reference Material Certificates of Analysis [47]. The absorbance of the particles was measured before and after functionalization with PEG ligands. These measurements permit corrections to be made for the decrease in absorbance amplitudes for the PEG-functionalized particles that account for loss of material on the filter and for spectral broadening from the presence of the PEG on the particle surface. Spectra of SH-PEG-methyl functionalized nanoparticles were used to find appropriate correction factors to account for broadening of spectra after functionalization. Because HS-PEG-methyl is transparent in the visible region, and it changed the shape of the gold nanoparticle spectra in the same way as the PEG-FITC ligands, known amounts of reference material were added to volumetric flasks with a large stoichiometric excess of HS-PEG-methyl. The samples were diluted to 5.00 mL and the maximum absorbance values were measured. The absorbance for the 10 nm sample was 79.9 ± 0.4 % of the value that was expected if the citrate-stabilized particles had been diluted with water alone. The 30 nm sample had an absorbance value that was 85.6 ± 0.3 % of the expected value if the sample had merely been diluted. The validity of these numbers was checked by measuring the absorbance spectra of all the fluorescently labeled particles before the unbound PEG ligands were removed—when the gold concentrations were still known—and subtracting the signal arising from the excess fluorescent PEG by spectral editing. The PEG-FITC functionalized particles were diluted to have absorbance values between 0.1 A. U. and 0.2 A. U. and were compared to a standard curve. The standard curves, including the best-fit lines, and unknown points are shown in Fig. S1 in the Electronic Supplementary Material (ESM).

Fluorescence Fluorescence was measured on a Synergy HT plate reader (BioTek Instruments, Winooski, VT). Three 100 μ L aliquots of each sample and standard were transferred to a clear-bottom, black, 96-well assay plate. Measurements were made with a 485/20 excitation filter and a 516/20 emission filter. Because the gold particles quench the fluorescence of the PEG-FITC, the PEG ligands were displaced from the gold particles, and the flocculated particles were removed by

centrifugation. Using the procedure described in [23] as a guide, the PEG was displaced from the particles in a 0.5 mol/L dithiothreitol (DTT), phosphate buffered saline (PBS), pH 8.0 solution: 100 μ L of PEGylated particles were diluted with 100 μ L of water and combined with 200 μ L of 1.0 mol/L DTT in pH 8.0 PBS (2X: 274 mmol/L NaCl, 5.4 mmol/L KCl, 23.8 mmol/L phosphate buffer). The samples were protected from light and incubated for 5 days. With the exception of the 10 nm-LA-PEG-FITC sample, all of the gold nanoparticles precipitated out of solution as determined by the absence of red color in solution and the formation of solid black flecks. Because a faint red color persisted in the 10 nm-LA-PEG-FITC sample, additional DTT was added to each sample to help ensure complete displacement. An additional 100 μ L of the 1.0 mol/L DTT solution was added to the 10 nm-LA-PEG-FITC sample and an additional 50 μ L was added to each of the other three samples. After an overnight incubation, no red color was observed, and water was added to each sample in equivalent amounts as the additional DTT volumes. The fluorescence in the supernatants was observable by eye in all four samples. The concentrations of the fluorescent ligands were determined by comparison to a set of standards that were prepared to have the same pH, ionic strength, and DTT concentrations as the unknowns.

Microscale thermogravimetric analysis Microscale thermogravimetric analysis (μ -TGA) techniques were previously reported [8, 29]. Briefly, for each sample, 10 μ L aliquots of the nanoparticle dispersions were deposited onto six ($n=6$) QCMs and heated in a muffle furnace to temperatures of interest. A measurement was made after heating to 100 $^{\circ}$ C, followed by successive measurements up to 600 $^{\circ}$ C in 100 $^{\circ}$ C increments with a standard impedance analyzer. Each measurement was corrected for changes in the quartz that occur with heating and excess water in the sample, as described previously. All QCMs were modified with a glass layer to prevent interactions between the gold nanoparticle samples and the gold electrodes at elevated temperatures.

MALDI MALDI-TOF-MS was used to determine the molecular weights of the PEG derivatives. 1 μ L of 0.5 mg/mL LA-PEG-NH₃ was combined with 5 μ L of 10 mg/mL 2,5-dihydroxybenzoic acid, and 1 μ L of 0.5 mg/mL HS-PEG-FITC was combined with 5 μ L of 10 mg/mL α -cyano-4-hydroxy cinnamic acid (α -CHCA). All of the solutions were in water, with the exception of α -CHCA, which was in a 1:1 mixture of water and acetonitrile, by volume. 0.5 μ L of each sample was deposited on a MALDI plate and analyzed on a Voyager-DE STR Biospectrometry Workstation (PerSeptive Biosystems, Framingham, MA).

Results and discussion

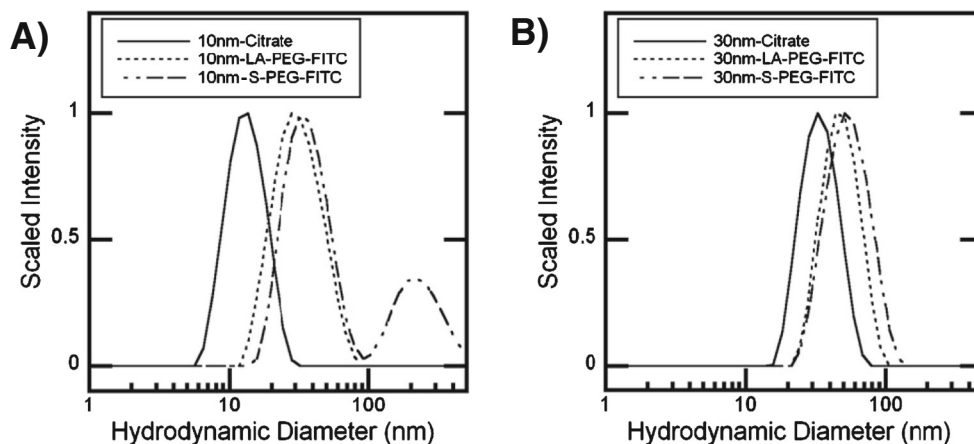
The formation of PEG layers on the gold surfaces is a well-known procedure, but must be verified. In this case, UV-vis spectroscopy and DLS were used to measure the PEG coating on the gold nanoparticles. Figure 1 compares the DLS signals of the citrate-stabilized nanoparticles with those of the nanoparticles stabilized with the PEG derivatives. The Z-average diameter for the 10 nm particles increased from 12.3 to 28.6 nm for the LA-PEG-FITC sample and to 53.5 nm for the HS-PEG-FITC sample. The much larger size measurement for the thiolate bound sample is due to the formation of a small population of flocs as evidenced by the peak above 100 nm. A more accurate assessment of size in this case comes from the peak maximum of the dominant peak in the HS-PEG-FITC sample from a non-negative least squares regularization algorithm [53]. The HS-PEG-FITC dominant peak is at 37.7 nm compared to a peak maximum of 32.8 nm for the LA-PEG-FITC sample. Despite the unmistakable signature of floc formation in this sample, the overwhelming majority of the sample remains suspended as individual particles. The substantial intensity of the floc peak arises because the scattering intensity varies as d^6 [6], where d is the particle diameter. By assuming that the refractive indexes of the flocs and the dispersed monomers were equal, the number of particles confined to flocs was estimated to be 0.004 % [54]. The Z-average diameter for the 30 nm particles shifts from 29.4 to 41.4 nm for the LA-PEG-FITC sample and to 45.9 nm for the HS-PEG-FITC sample. No flocs were observed in the 30 nm samples. For particles of both sizes, the hydrodynamic radii were greater for the particles functionalized with HS-PEG-FITC than for the particles functionalized with LA-PEG-FITC.

The UV-vis spectra for citrate-stabilized and PEG-stabilized are shown in Fig. 2. Upon functionalization with PEG, the spectra are red-shifted and broadened, which is consistent with the addition of a ligand to the gold surface [15, 27, 55]. Only the LA-PEG-FITC spectra are shown in Fig. 2 since the HS-PEG-FITC spectra have identical shapes. Peak shapes of these spectra also match the shape of spectra for particles functionalized with HS-PEG-methyl where the PEG had a larger average molecular weight (5,000 g/mol). The peak maxima (λ_{\max}) for PEG-functionalized 30 nm particles were each red-shifted from 526 to 528 nm, and the 10 nm spectra were also red-shifted by 2 from 516 to 518 nm. No absorbance peaks above 600 nm were observed, which is further evidence that there was not a significant number of flocs in the 10 nm-S-PEG-FITC sample [55].

UV-vis spectra were used to determine the concentration of the PEG-functionalized particles by use of the size and gold mass fraction data from the NIST Certificates of Analysis [47], which are summarized in Table 1.

The maximum absorbances for the spectra were adjusted by their corresponding correction factors (0.799^{-1} for the

Fig. 1 DLS intensity particle size distributions for citrate- and PEG-stabilized **a** 10 and **b** 30 nm particles



10 nm PEGylated particles and 85.6^{-1} for the 30 nm particles), and the concentrations of gold were calculated as a percentage of the undiluted, unfiltered, and un-functionalized reference material concentrations. To report a concentration in units of moles of particles per liter would be misleading in this case, because it would force a choice to be made on the size of the particles; and as can be seen in Table 1, different measurement techniques give different values of sizes, since they measure different size parameters. A concentration (μg of gold / g nanoparticle sample) was determined by using the concentration of the particles in percentage units by the gold mass-fraction. The undiluted concentrations of gold nanoparticles were determined to be $(133.0 \pm 6.7) \mu\text{g/g}$ for the 10 nm-LA-PEG-FITC sample, $(79.9 \pm 3.6) \mu\text{g/g}$ for the 10 nm-S-PEG-FITC sample, $(251.1 \pm 4.1) \mu\text{g/g}$ for the 30 nm-LA-PEG-FITC sample, and $(223.3 \pm 4.1) \mu\text{g/g}$ for the 30 nm-S-PEG-FITC sample. The lower concentrations of the 10 nm samples than the 30 nm samples are due to a larger loss of material from the centrifugation cycles. The uncertainty in the concentrations of the particles was propagated from the uncertainty in the concentration from the standard curve—which

incorporates interdependence of the slope and the intercept of the best fit line [56] and the uncertainties in the correction factors and Au mass fraction.

The fluorescence calibration plots shown in Fig. S1 in the ESM were used to find the concentrations of the displaced ligands, from which the concentrations of bound ligands in the original, undiluted samples were calculated to be $(10.13 \pm 0.08) \mu\text{g/g}$ for the 10 nm-LA-PEG-FITC sample, $(23.1 \pm 0.3) \mu\text{g/g}$ for the 10 nm-S-PEG-FITC sample, $(1.25 \pm 0.07) \mu\text{g/g}$ for the 30 nm-LA-PEG-FITC sample, and $(5.66 \pm 0.07) \mu\text{g/g}$ for the 30 nm-S-PEG-FITC sample. Uncertainties were determined analogously to the uncertainties for the gold concentrations. Gold nanoparticle and PEG concentrations were both kept in units of mass so that the mass percentage of gold could be easily calculated without the need for information on nanoparticle sizes and PEG molecular weights.

Because traditional TGA uses excessive amounts of material (at least 1 mg per sample) μ -TGA was used to evaluate the amount of PEG bound to the gold nanoparticles. Microscale thermogravimetric analysis allows for samples of 1–10 μg to be analyzed using a quartz crystal microbalance that is heated

Fig. 2 UV-vis spectra for citrate- and PEG-stabilized **a** 10 and **b** 30 nm particles. The spectra were scaled to have peak maxima equal to 1 for comparison

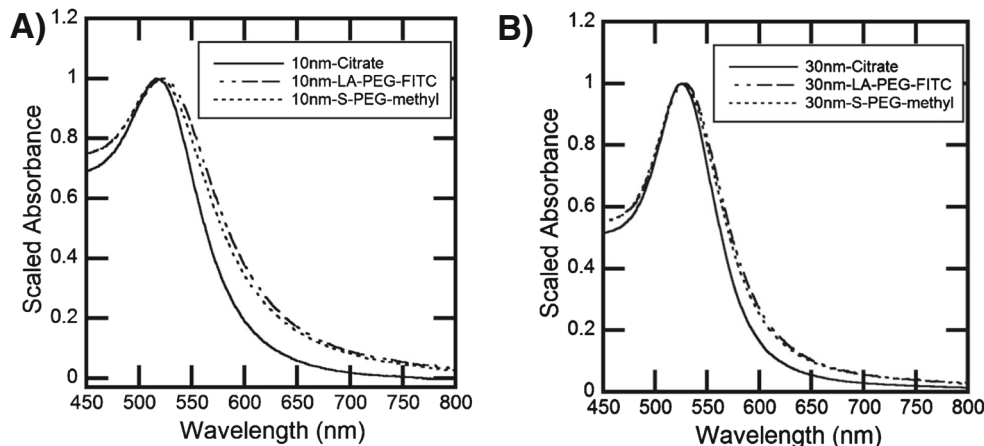


Table 1 NIST Values for 10 and 30 nm Gold Nanoparticle Standard Reference Materials [47]

	10 nm (SRM 8011)	30 nm (SRM 8012)
Technique	Particle Size (nm)	Particle Size (nm)
Atomic force microscopy	8.5±0.3	24.9±1.1
Scanning electron microscopy	9.9±0.1	26.9±0.1
Transmission electron microscopy	8.9±0.1	27.6±2.1
Differential mobility analysis	11.3±0.1	28.4±1.1
DLS (173° scattering angle)	13.5±0.1	28.6±0.9
Small-angle X-ray scattering	9.1±1.8	24.9±1.2
ICP-OES	Au mass fraction (µg/g) 51.56±0.23	Au mass fraction (µg/g) 48.17±0.33

every 100 °C to 600 °C. In the resulting thermograms (Fig. 3) a mass loss event is observed between 200 and 400 °C. At temperatures higher than 500 °C, a mass gain is observed in the μ -TGA curve (not shown), indicating the sample is taking on mass. This increase has previously been observed for gold nanoparticles [8] but is not of concern for determining PEG concentration, as the ligand decomposes at lower temperatures; all of the samples were heated well past the reported decomposition temperature of 318 °C for PEG [24]. The

measured mass loss at 400 °C is shown in Table 2, along with values that would be expected for mass loss from the UV-vis and fluorescence measurements.

The large uncertainties in the μ -TGA measurements are due to inconsistent decomposition of the sample at a given temperature. The results are clearly different from the values predicted from the fluorescence method (Table 2). The fluorescence measurements rely on ligand displacement from the gold surface. In this case, it is possible the ligands are not fully

Fig. 3 μ -TGA data for PEGylated gold samples with curve fits. The error bars represent the standard deviations of the measurements ($n=6$)

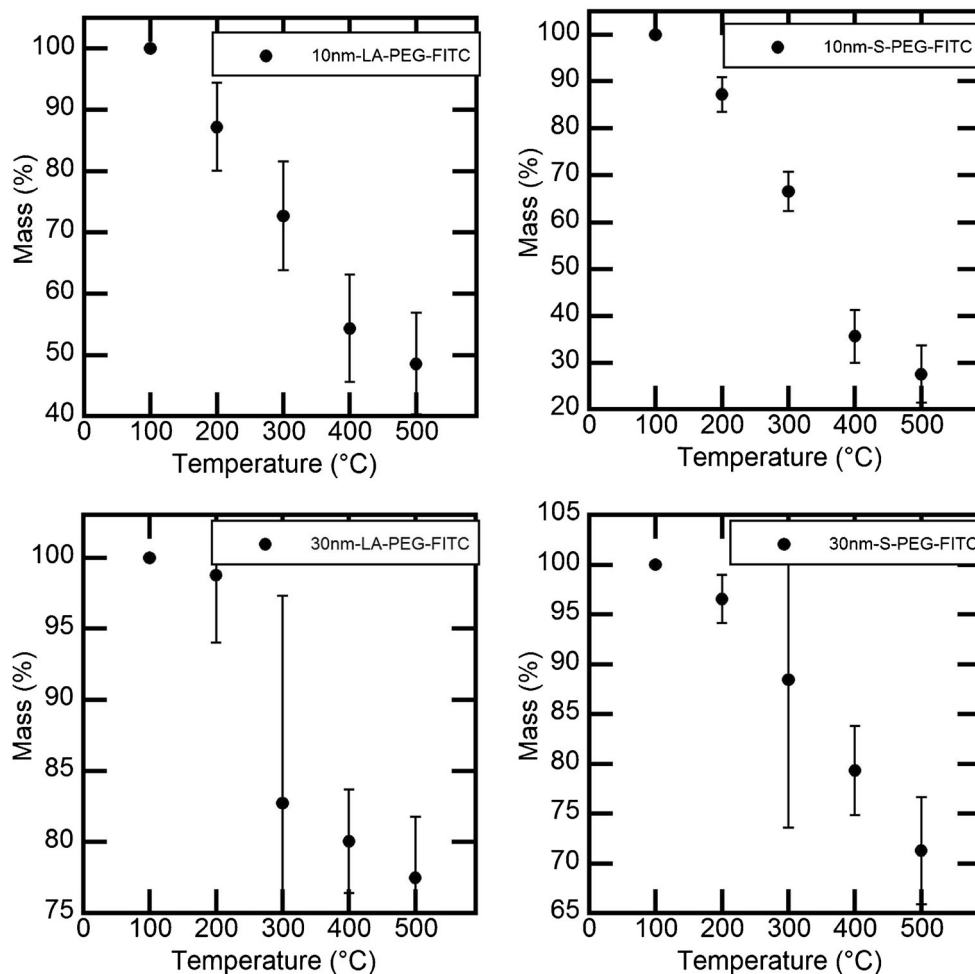


Table 2 Predicted and Measured Mass Au in Sample

Sample	Fluorescence Mass (%)	μ -TGA Mass (%)
10 nm-LA-PEG-FITC	93.0 \pm 6.4	48.6 \pm 8.3
10 nm-S-PEG-FITC	77.5 \pm 4.4	27.6 \pm 6.1
30 nm-LA-PEG-FITC	99.5 \pm 2.2	77.5 \pm 4.3
30 nm-S-PEG-FITC	97.5 \pm 2.4	71.3 \pm 5.4

dissociated and the value reported is artificially high. The μ -TGA measurement assumes the decomposition of everything except for the gold. Any organic matter destroyed at temperatures less than 400 °C would be burned off, including water, ligands and any products left behind from the synthesis process. The remaining mass is assumed to be gold and its oxidation products, which would potentially increase the mass % remaining. In this case, it is expected the oxidation would not have an effect in the 400 °C measurement. To compare these data to results obtained by others, the mass percent data were converted to the average area occupied per ligand, i.e., a footprint size. The nanoparticles were approximated as spheres, and the TEM data from the Certificates of Analysis [47] were used to approximate particle diameters. Molecular weights of the PEG ligands were obtained with MALDI-TOF-MS. Data for LA-PEG-NH₃ and HS-PEG-FITC with Gaussian curve fits are shown in Fig. 4. The supplier's molecular weight specifications were 3,400 g/mol for both LA-PEG-NH₃ and HS-PEG-FITC. The average molecular weights from the peak centers of the Gaussian fits were determined to be 3,900 g/mol for LA-PEG-FITC and 3,850 g/mol for HS-PEG-FITC. The LA-PEG-FITC was not measured directly, because it did not ionize adequately for MALDI analysis; therefore, 289 g/mol was added to the LA-PEG-NH₃ peak to compensate for the addition of the fluorophore. The footprint sizes determined from this research along with a non-exhaustive list of footprint sizes calculated from other laboratories are tabulated in Table 3. Anytime a footprint size is calculated, there is a need

to make assumptions about how the molecule is oriented once absorbed or reacted to a surface. There will be new equilibria effects including entanglement of the ligands, competitive affinities, or hydrophobic interactions. This paper assumes the calculation of complete coverage of evenly distributed ligands. The footprint sizes calculated from the fluorescence measurements are comparable to those measured by others with the same technique (Table 3); although there is wide variability based on the different ligands and particle sizes used most of the footprint sizes calculated from fluorescence measurements fall in the 2–10 nm² range. There is a vast difference between the measured fluorescence and μ -TGA footprint sizes determined in this work (Table 3). The differences between the results are greater for the 30 nm particles than the 10 nm particles and for the lipoic acid samples than the thiolate samples.

The differences in these data indicate how the two analytical methods may provide different results, as is seen for many situations where methods are used to determine nanoparticle properties (i.e., Table 1) [47]. It is possible that the DTT treatment did not displace all of the bound ligands from the gold surfaces and that a lower percentage of lipoic acid ligands were displaced than thiolates, which would be consistent with the greater stability of multi-dentate ligands reported in the literature [9, 50, 59–64]. This stability is seen despite indications that the lipoic acid-gold bond is weaker than a thiolate linkage [65], and that the grafting density of the lipoic acid ligands is less than the density of the thiolate ligands, shown here. With a weaker linkage to gold and a lower surface coverage, the increased stability may arise from the short alkane chain on lipoic acid, which could create a hydrophobic region near the gold core. Furthermore, the higher footprint size of the lipoic acid ligands may allow the PEG to adopt a more compact structure near the gold core, which could create a greater barrier to external agents than ligands in an extended conformation. This explanation would also account for the lower hydrodynamic diameters observed in the DLS measurements for the lipoic acid ligands [53]. The greater stability

Fig. 4 MALDI-TOF-MS data (solid, black lines) with Gaussian fits (red, dashed lines) for **a** HS-PEG-FITC and **b** LA-PEG-NH₃

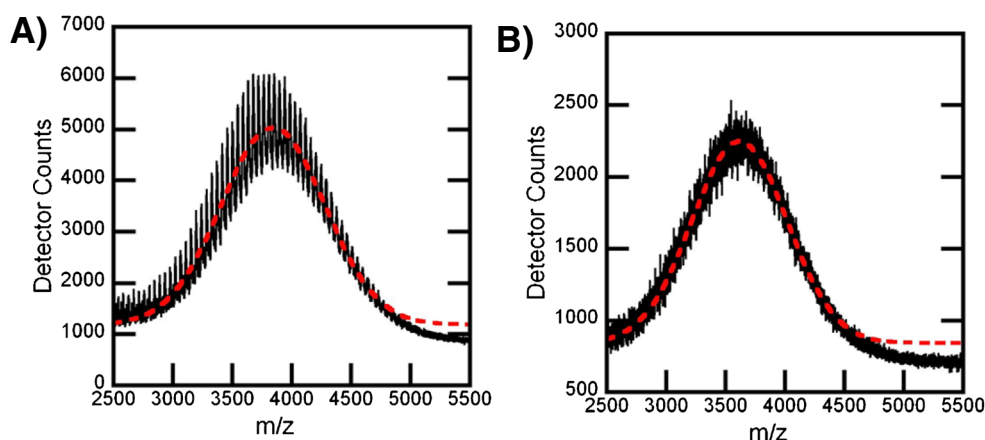


Table 3 Comparison of ligand footprint sizes on gold

Particle Diameter (nm)	Ligand	Technique	Footprint Size (nm ²)
8.9*	LA-PEG-FITC, HS-PEG-FITC	Fluorescence	3.0, 0.77
27.6*	LA-PEG-FITC, HS-PEG-FITC	Fluorescence	14.53, 2.81
15, 30, 50, 80, 150, 250 [23]	SH-A ₁₀ -DNA-FAM SH-T ₁₀ -DNA-FAM SH-PEG-DNA-FAM	Fluorescence	8.67, 8.71, 9.80, 8.76, 9.86, 11.92 4.37, 4.75, 8.78, 8.25, 9.12, 10.61 2.97, 3.47, 6.35, 6.11, 9.04, 8.14
8.9*	LA-PEG-FITC, HS-PEG-FITC	μ-TGA	0.21, 0.08
27.6*	LA-PEG-FITC, HS-PEG-FITC	μ-TGA	0.25, 0.18
20 [20]	S-PEG-Lactose, S-PEG-acetal (MW 6000)	TGA	2.42
5.2 [24]	mPEG-thiol (5000 g/mol)	TGA	0.35
2.4 [25]	S-(CH ₂) _n -CH ₃ , n=7, 11, 15	TGA	0.144 (sphere), 0.190 (cuboctahedron)
4.9 [26]	mPEG-thiol (2000 g/mol)	TGA	1.26 (inscribed sphere), 1.42 (circumscribed sphere)
5.4, 5.7, 5.3, 5.2 [27] 12.4, 11.9, 11.0, 12.2 18.7, 19.9, 17.6, 17.3	PtBA-2680,PDMDOMAA-5060, PBAEAM-5390, PNIPAM-5110	TGA	1.05, 1.07, 5.52, 1.23 1.40, 0.97, 0.67, 1.04 1.22, 0.70, 0.49, 0.75
2 [28]	Hexaethylene glycol paclitaxel linked to 4 mercaptophenol functionalized particles	TGA	0.108 (4-mercaptophenol), 0.163 (paclitaxel)
Au(111) surface [57]	docosyl mercaptan	Electron Diffraction	2.14
2.5–12.5 [58]	S-(CH ₂) _n -CH ₃ , n=7, 11, 16	Theory	1.6–2.7

Data from this report

observed for the 30 nm particles over the 10 nm particles, however, may indeed be due to steric effects, since the greater curvature of the 10 nm particles can allow greater access to the gold surface. Without a direct measurement, it is difficult to determine the orientation and physical state of the attached ligands.

The μ-TGA results are within the expected uncertainty of results for ligand density coverages obtained by traditional TGA. Over a wide variety of ligands and particle sizes footprint sizes calculated from TGA tend to fall between 0.1 and 1.5 nm² (Table 3). These data comparisons and the previous demonstration that this technique correlates with TGA for other sample types [29], provide strong evidence that the μ-TGA measurements are dependable. The higher footprint sizes from the fluorescence measurements in this system may be accounted for if all of the ligands were released into solution from the gold surface. These results may vary based on the size of the gold nanoparticles and surface ligands used (Table 3). An interesting result is that the footprint sizes of the lipoic acid ligands indicate they could be larger than the thiolate ligands and the ligands may be more densely spaced on the smaller particles. The μ-TGA results also assume that all material that comes off the surface can be attributed to the ligands. The majority of the water is accounted for in the beginning, but it is possible that associated water and other products of the synthesis may exist.

Conclusions

As particle sizes reach the nanoscale, the molecules bound to the particle surface compose a significant portion of their mass. In this report, we used this attribute to demonstrate the measurement of PEG surface densities on gold nanoparticle Standard Reference Materials with minimal sample destruction by use of μ-TGA and fluorescence spectrometry. It was shown that μ-TGA is a convenient technique for the quantification of ligands bound to inorganic particles while sacrificing a minimal amount of sample, and the treatment of the functionalized nanoparticle dispersions with dithiothreitol may be insufficient to achieve complete displacement of the surface ligands for quantification by fluorescence measurements. Footprint sizes measured by fluorescence displacement show a marked increase in size from those measured by μ-TGA. The lower surface densities determined from the fluorescence measurements may be due to incomplete displacement of the ligands from the gold surfaces. Demers et al. [22] provided strong evidence that their fluorescent ligands were displaced completely by mercaptoethanol by comparing the fluorescence signal from the displacement reaction to the fluorescence signal obtained by dissolving the gold cores with cyanide. However, every particle and displacement scheme is different. We stress that any measurements of ligand concentrations that are made by displacing the ligands from the

nanoparticles need to demonstrate that complete displacement was achieved. The μ -TGA measurements were made with inexpensive equipment—a muffle furnace and an impedance analyzer—and required no special expertise. Although measurements were taken at enough temperatures to mimic a TGA curve, this is not required for the determination of surface coverage, as only the initial and final masses are needed. This technique has been studied further to reduce uncertainties and eliminate the need for external heating by incorporating an onboard heater on the QCMs. The μ -TGA technique could be a method to quantify bound organic ligands to a broad range of inorganic nanoparticles with small volumes.

Acknowledgments Karl Sebby gratefully acknowledges the NRC Research Associateship Program for funding.

References

- Cheng MM, Cuda G, Bunimovich YL, Gaspari M, Heath JR, Hill HD, Mirkin CA, Nijdam AJ, Terracciano R, Thundat T, Ferrari M (2006) *Curr Opin Chem Biol* 10:11–19
- Petros RA, DeSimone JM (2010) *Nat Rev Drug Discov* 9:615–627
- Oberdörster G, Maynard A, Donaldson K, Castranova V, Fitzpatrick J, Ausman KD, Carter J, Karn B, Kreyling W, Lai D, Olin S, Monteiro-Riviere NA, Warheit DB, Yang H (2005) *Part Fibre Toxicol* 2:1–35
- Boverhof DR, David RM (2009) *Anal Bioanal Chem* 396:953–961
- Richman EK, Hutchison JE (2009) *ACS Nano* 3:2441–2446
- Grainger DW, Castner DG (2008) *Adv Mater* 20:867–877
- Hall JB, Dobrovolskaia MA, Patri AK, McNeil SE (2007) *Nanomed* 2:789–803
- Mansfield E, Tyner KM, Poling CM, Blacklock JL (2014) *Anal Chem* 86:1478–1484
- Jones CF, Grainger DW (2009) *Adv Drug Deliv Rev* 61:438–456
- Kroll A, Pillukat MH, Hahn D, Schneidenburger J (2009) *Eur J Pharm Biopharm* 72:370–377
- Shaw SY, Westly EC, Pittet MJ, Subramanian A, Schreiber SL (2008) *Weissleder. R Proc Natl Acad Sci U S A* 105:7387
- Fischer HC, Chan WC (2007) *Curr Opin Biotechnol* 18:565–571
- Linkov I, Satterstrom FK, Corey LM (2008) *Nanomed Nanotechnol Biol Med* 4:167–171
- Nel AE, Madler L, Velegol D, Xia T, Hoek EMV, Somasundaran P, Klaessig F, Castranova V, Thompson M (2009) *Nat Mater* 8:543–557
- Casals E, Pfäller T, Duschl A, Oostingh GJ, Puntès V (2010) *ACS Nano* 4:3623–3632
- Baer DR, Gaspar DJ, Nachimuthu P, Techane SD, Castner DG (2010) *Anal Bioanal Chem* 396:983–1002
- Zhang B, Yan B (2010) *Anal Bioanal Chem* 396:973–982
- MacCuspie RI, Rogers K, Patra M, Suo Z, Allen AJ, Martin MN, Hackley VA (2011) *J Environ Monit* 13:1212
- Dobrovolskaia MA, McNeil SE (2007) *Nat Nanotechnol* 2:469–478
- Takae S, Akiyama Y, Otsuka H, Nakamura T, Nagasaki Y, Kataoka K (2005) *Biomacromolecules* 6:818–824
- Pease LF, Tsai D-H, Zangmeister RA, Zachariah MR, Tarlov MJ (2007) *J Phys Chem C* 111:17155–17157
- Demers LM, Mirkin CA, Mucic RC, Reynolds RA, Letsinger RL, Elghanian R, Viswanadham G (2000) *Anal Chem* 72:5535–5541
- Hurst SJ, Lytton-Jean AKR, Mirkin CA (2006) *Anal Chem* 78:8313–8318
- Wuelfing WP, Gross SM, Miles DT, Murray RWJ (1998) *Am Chem Soc* 120:12696–12697
- Terrill RH, Postlethwaite TA, Chen C, Poon CD, Terzis A, Chen A, Hutchison JE, Clark MR, Wignall GJ (1995) *Am Chem Soc* 117:12537–12548
- Maccarini M, Briganti G, Rucareanu S, Lui XD, Sinibaldi R, Sztucki M, Lennox RBJ (2010) *Phys Chem C* 114:6937–6943
- Liang M, Lin IC, Whittaker MR, Minchin RF, Monteiro MJ, Toth I (2009) *ACS Nano* 4:403–413
- Gibson JD, Khanal BP, Zubarev ERJ (2007) *Am Chem Soc* 129:11653–11661
- Mansfield E, Kar A, Quinn TP, Hooker SA (2010) *Anal Chem* 82:9977–9982
- Boisselier E, Astruc D (2009) *Chem Soc Rev* 38:1759
- Cobley CM, Chen J, Cho EC, Wang LV, Xia Y (2011) *Chem Soc Rev* 40:44
- Arviso R, Bhattacharya R, Mukherjee P (2010) *Expert Opin Drug Deliv* 7:753–763
- Han G, Ghosh P, Rotello VM (2007) *Nanomed* 2:113–123
- Paciotti GF, Myer L, Weinreich D, Goia D, Pavel N, McLaughlin RE, Tamarkin L (2004) *Drug Delivery* 11:169–183
- Yang P-H, Sun X, Chiu J-F, Sun H, He Q-Y (2005) *Bioconjugate Chem* 16:494–496
- Kim C, Agasti SS, Zhu Z, Isaacs L, Rotello VM (2010) *Nature Chem* 2:962–966
- Brown SD, Nativo P, Smith J-A, Stirling D, Edwards PR, Venugopal B, Flint DJ, Plumb JA, Graham D, Wheate NJJ (2010) *Am Chem Soc* 132:4678–4684
- Pissuwan D, Niidome T, Cortie MJB (2011) *Control Release* 149:65–71
- Han G, You CC, Kim BJ, Turingan RS, Forbes NS, Martin CT, Rotello VM (2006) *Angew Chem Int Ed Engl* 45:3165–3169
- Ghosh P, Han G, De M, Kim CK, Rotello VM (2008) *Adv Drug Deliv Rev* 60:1307–1315
- Thomas M, Klibanov AM (2003) *Proc Natl Acad Sci U S A* 100:9138
- Baptista P, Pereira E, Eaton P, Doria G, Miranda A, Gomes I, Quaresma P, Franco R (2008) *Anal Bioanal Chem* 391:943–950
- Elghanian R (1997) *Science* 277:1078–1081
- Huang XH, Jain PK, El-Sayed IH, El-Sayed MA (2008) *Lasers Med Sci* 23:217–228
- Liao H, Nehl CL, Hafner JH (2006) *Nanomed* 1:201–208
- Examples include technologies developed by Cytimmune and Nanosphere.
- Kaiser DL, Watters RL Jr (2007) Report of investigation: gold nanoparticles, nominal 10 nm diameter; RM 8011. National Institute of Standards and Technology, Gaithersburg, MD, p 10, 20899
- Niidome T, Yamagata M, Okamoto Y, Akiyama Y, Takahashi H, Kawano T, Katayama Y, Niidome YJ (2006) *Control Release* 114:343–347
- Shenoy D, Fu W, Li J, Crasto C, Jones G, DiMarzio C, Sridhar S, Amiji M (2006) *Int J Nanomed* 1:51
- Zhang G, Yang Z, Lu W, Zhang R, Huang Q, Tian M, Li L, Liang D, Li C (2009) *Biomaterials* 30:1928–1936
- Kang B, Mackey MA, El-Sayed MAJ (2010) *Am Chem Soc* 132:1517–1519
- Certain commercial equipment, instruments, or materials are identified in this document. Such identification implies neither recommendation nor endorsement by the National Institute of Standards and Technology, nor that the products identified are necessarily the best available for the purpose.

53. Tsai D-H, DelRio FW, MacCuspie RI, Cho TJ, Zachariah MR, Hackley VA (2010) *Langmuir* 26:10325–10333
54. Tsai D-H, DelRio FW, Keene AM, Tyner KM, MacCuspie RI, Cho TJ, Zachariah MR, Hackley VA (2011) *Langmuir* 27:2464–2477
55. Daniel M, Astruc D (2004) *Chem Rev* 104:293–346
56. Harris DC (1995) *Quantitative chemical analysis*, 4th edn. W.H. Freeman and Company, New York
57. Strong L, Whitesides GM (1988) *Langmuir* 4:546–558
58. Tambasco M, Kumar SK, Szleifer I (2008) *Langmuir* 24:8448–8451
59. Stewart MH, Susumu K, Mei BC, Medintz IL, Delehanty JB, Blanco-Canosa JB, Dawson PE, Mattoussi HJ (2010) *Am Chem Soc* 132:9804–9813
60. Mangeney C, Ferrage F, Aujard I, Marchi-Artzner V, Jullien L, Ouari O, Rékaï ED, Laschewsky A, Vikholm I, Sadowski JWJ (2002) *Am Chem Soc* 124:5811–5821
61. Li Z, Jin R, Mirkin CA, Letsinger RL (2002) *Nucleic Acids Res* 30:1558–1562
62. Letsinger RL, Elghanian R, Viswanadham G, Mirkin CA (2000) *Bioconjug Chem* 11:289–291
63. Dougan JA, Karlsson C, Smith WE, Graham D (2007) *Nucleic Acids Res* 35:3668–3675
64. Dixit V, Van den Bossche J, Sherman DM, Thompson DH, Andres RP (2006) *Bioconjug Chem* 17:603–609
65. Langry KC, Ratto TV, Rudd RE, McElfresh MW (2005) *Langmuir* 21:12064–12067